Geomechanical stability of the caprock during CO_2 sequestration in deep saline aquifers

Victor Vilarrasa[a,b] 1*, Sebastia Olivella[b], Jesus Carrera[a]

[a]*Hydrogeology Group (GHS), Institute of Environmental Assessment & Water Research (IDAEA), Jordi Girona 18-26, Barcelona, 08034, Spain*
[b]*Department of Geotechnical Engineering and Geosciences, Technical University of Catalonia (UPC), Jordi Girona 1-3, Barcelona 08034, Spain*

Abstract

Sequestration of carbon dioxide (CO_2) in deep saline aquifers has emerged as a mitigation strategy for reducing greenhouse gas emissions to the atmosphere. The large amounts of supercritical CO_2 that need to be injected into deep saline aquifers may cause large fluid pressure buildup. The resulting overpressure will produce changes in the effective stress field. This will deform the rock and may promote reactivation of sealed fractures or the creation of new ones in the caprock seal, which could lead to escape paths for CO_2. To understand these coupled hydromechanical phenomena, we model an axisymmetric horizontal aquifer-caprock system. We study plastic strain propagation patterns using a viscoplastic approach. Simulations illustrate that plastic strain may propagate through the whole thickness of the caprock if horizontal stress is lower than vertical stress. In contrast, plastic strain concentrates in the contact between the aquifer and the caprock if horizontal stress is larger than vertical stress. Aquifers that present a low-permeability boundary experience an additional fluid pressure increase once the pressure buildup cone reaches the outer boundary. However, fluid pressure does not evolve uniformly in the aquifer. While it increases in the low-permeability boundary, it drops in the vicinity of the injection well because of the lower viscosity of CO_2. Thus, caprock stability does not get worse in semi-closed aquifers compared to open aquifers. Overall, the caprock acts as a plate that bends because of pressure buildup, producing a horizontal extension of the upper part of the caprock. This implies a vertical compression of this zone, which may produce settlements instead of uplift in low-permeability ($k \leq 10^{-18}$ m^2) caprocks at early times of injection.

Keywords: Pressure buildup; hydromechanical coupling; dilatancy; fracture; stress state

1. Introduction

Carbon dioxide (CO_2) sequestration in deep saline aquifers represents a promising mitigation strategy for the reduction of CO_2 emissions to the atmosphere. CO_2 is injected in a supercritical state, ensuring an efficient storage due to its relatively high density. CO_2, though, will be lighter than the resident brine. Therefore, the vertical component of its flow will be large because of buoyancy. Hence, suitable aquifers should be capped by a low-permeability rock, or caprock, to avoid CO_2 migration to upper aquifers and the surface. This caprock may undergo large pressure buildup because of CO_2 injection. This will affect the stress field and may induce large deformations [1, 2], which can eventually damage the caprock and open up new flow paths. To study this, the flow and the mechanical problems have to be solved together, leading to the hydromechanical coupling.

Solving the hydromechanical coupling numerically is necessary for determining the conditions under which mechanical failure (shear failure or hydraulic fracture) could occur. There are several evidences supporting this: (i) simplified analytical solutions often predict incorrect values of the fracturing pressure [3, 4]; (ii) purely hydraulic simulations fail to predict the response of fluid pressure in the caprock (they predict an immediate increase while it actually drops at the beginning of injection because of dilatancy) [5]; and (iii) purely hydraulic codes cannot simulate the effect of the initial stress state, which affects significantly the failure behavior [6, 7].

Strains are induced by pressure buildup evolution, which depends on the hydraulic boundary conditions. In open aquifers the displaced brine can easily migrate out laterally [8]. This limits pressure buildup, but may salinize freshwater bodies [5]. In contrast, closed and semi-closed aquifers experience an additional pressure buildup, limiting the CO_2 injection capacity, which will be controlled by rock and fluid compressibility [9, 10]. This additional overpressure, which may compromise caprock stability, depends on the permeability of the caprock. Relatively permeable caprocks (permeability higher than 10^{-18} m^2) diminish pressure buildup because brine can leak through them [8, 9]. Previous hydromechanical studies simulate open aquifers [7] and even aquifers crossed by a

---

* Corresponding author. Tel.: +34-93-405-41-69.
E-mail address: victor.vilarrasa@upc.edu.

sealed fault that opens up with increasing pressure buildup [3], but an aquifer completely surrounded by low-permeability boundaries has not yet been investigated.

The aim of this paper is to analyze the effect of the initial stress state and hydraulic boundary condition on the failure mechanisms that may occur in the caprock, depending on its permeability. To this end, we use a viscoplastic approach, so that failure mechanisms can be observed.

2. Methods

2.1. Geometry and boundary conditions

An ideal homogeneous horizontal aquifer-caprock system is considered for this study (Figure 1). The top of the 100 m thick aquifer is located at a depth of 1000 m. The aquifer is overlaid by a 400 m thick low-permeability caprock. The caprock is covered by 600 m of low shear strength geological material, which is represented by an equivalent overburden. The system is axisymmetric and extends laterally 20 km. An injection well with a radius of 150 mm is placed at the centre of the domain.

The properties of the aquifer and caprock correspond to those of permeable sandstone and shale, respectively (Table 1). The initial conditions are: hydrostatic pressure and constant temperature of $T=320$ K. CO_2 is injected uniformly throughout the entire thickness of the aquifer at a constant rate of 113 kg/s (3.6 Mt/yr). In order to model open aquifers a constant head boundary condition is imposed at the outer boundary. Semi-closed aquifers are modeled with a mixed or Cauchy boundary condition at the outer boundary. The mechanical boundary conditions are zero normal displacement on the bottom and outer boundaries. A constant, vertical lithostatic stress is imposed on the top of the caprock. The initial stress fields can display either a larger vertical stress than horizontal stress or a larger horizontal than vertical stress. The values used for this study are $\sigma_h = 0.85\sigma_v$ and $\sigma_h = 1.5\sigma_v$, where σ_h is the horizontal stress and σ_v is the lithostatic stress.
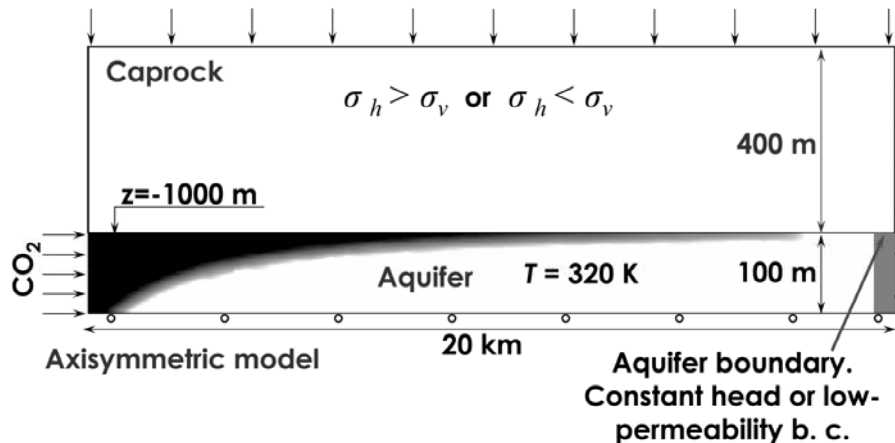

Figure 1. Schematic description of the model geometry and boundary conditions

Table 1.- Material properties used in the hydromechanical analysis of the aquifer-caprock system

Property	Aquifer	Caprock
Young's Modulus, E (MPa)	$1 \cdot 10^4$	$5 \cdot 10^3$
Poisson's ratio, ν (−)	0.3	0.3
Porosity, ϕ (−)	0.1	0.01
Cohesion, c' (MPa)	0.01	0.01
Angle of friction, ϕ' (º)	30	21
Permeability, k (m^2)	10^{-13}	10^{-16} or 10^{-18}
Relative liquid permeability, k_{r_l} (−)	S_l^3	S_l^6
Relative gas permeability, k_{r_g} (−)	S_g^3	S_g^6
Gas entry pressure, P_0 (MPa)	0.02	0.6
van Genuchten m (−)	0.8	0.5

2.2. Hydromechanical coupling

Viscoplastic models give a realistic description of geologic materials behavior and are computationally advantageous for solving plasticity problems [11, 12]. Total strain can be divided into elastic and inelastic or viscoplastic strain

$$d\boldsymbol{\varepsilon} = d\boldsymbol{\varepsilon}^e + d\boldsymbol{\varepsilon}^i \qquad (1)$$

where $\boldsymbol{\varepsilon}^e$ is the elastic strain tensor and $\boldsymbol{\varepsilon}^i$ is the viscoplastic strain tensor.

While elastic strain is recoverable, viscoplastic strain is irreversible. The latter occurs when the stresses exceed a critical state at which the rock yields. This critical state is defined by a yield surface $F = 0$. Pure elasticity occurs while $F \leq 0$ and $F > 0$ implies viscoplastic strain. For the viscoplastic strain, we adopted a Drucker-Prager yield function. This viscoplastic model is explained in detail in [5].

Hooke's law relates the elastic strain with the effective stress as

$$\boldsymbol{\varepsilon}^e = \left(p'/3K\right)\mathbf{I} + 1/2G\left(\boldsymbol{\sigma}' - p'\mathbf{I}\right) \qquad (2)$$

where $\boldsymbol{\sigma}'$ is the effective stress tensor, $p' = \left(\sigma'_x + \sigma'_y + \sigma'_z\right)/3$ is the mean effective stress, $\mathbf{I}$ is the identity matrix, K is the bulk modulus and G is the shear modulus.

The inverse of Eq (2) gives the effective stress as a function of the elastic strain as

$$\boldsymbol{\sigma}' = K\varepsilon_v\mathbf{I} + 2G\left(\boldsymbol{\varepsilon}^e - \varepsilon_v/3\mathbf{I}\right) \qquad (3)$$

where $\varepsilon_v = \nabla \cdot \mathbf{u}$ is the volumetric strain and $\mathbf{u}$ is the displacement vector.

Considering the sign criterion of continuum mechanics, i.e. stress is positive in tension while fluid pressure is positive in compression, the effective stress tensor is defined as

$$\boldsymbol{\sigma}' = \boldsymbol{\sigma} + p_f \mathbf{I} \tag{4}$$

where $\boldsymbol{\sigma}$ is the total stress tensor and p_f is the fluid pressure.

For the solution of the mechanical problem, the momentum balance of the porous media has to be satisfied. If the inertial terms are neglected, this reduces to the equilibrium of stresses

$$\nabla \cdot \boldsymbol{\sigma} + \mathbf{b} = \mathbf{0} \tag{5}$$

where $\mathbf{b}$ is the vector of body forces.

Combining equations (3) and (4) and introducing them in (5), together with the compatibility relationship that relates strain with displacements as

$$\boldsymbol{\varepsilon} = 1/2 \left(\nabla \mathbf{u} + \left(\nabla \mathbf{u} \right)^T \right), \tag{6}$$

where the superscript *T* denotes transpose, the following elasticity equation is obtained

$$G \nabla^2 \mathbf{u} + \left((1/3)G + K \right) \nabla \left(\nabla \cdot \mathbf{u} \right) - \nabla p_f + \mathbf{b} = 0. \tag{7}$$

Equation (7) is coupled with the flow equation through the fluid pressure (third term). Assuming that there is no external loading and that the grains are incompressible, the mass conservation of the fluid can be written as

$$\phi \beta \, \partial p_f / \partial t + \mathrm{d}/\mathrm{d}t \left(\nabla \cdot \mathbf{u} \right) + \nabla \cdot \mathbf{q} = 0 \tag{8}$$

where ϕ is porosity, $\beta = (1/\rho)(\mathrm{d}\rho/\mathrm{d}p_f)$ is the compressibility of water, ρ is density, t is time, $\mathbf{q} = -(k/\mu)(\nabla p_f + \rho g \nabla z)$ is the water flux given by Darcy's law, k is permeability, μ is viscosity, g is gravity and z is the vertical coordinate.

Note that the flow equation (Eq (8)) is also coupled with the mechanical equation (Eq (7)) through the volumetric strain, i.e. the divergence of the displacements (second term).

2.3. Numerical solution

Equations (7) and (8) are solved together numerically to simulate the injection of CO_2 into a homogeneous saline aquifer. We use the finite element numerical code CODE_BRIGHT [13, 14] modified for CO_2 sequestration [5]. Quadrilateral elements are used to enable the calculation of the mechanical problem. The mesh is a combination of an unstructured mesh close to the injection well (first 2 km) and structured far from it. The elements located close to the injection well are of 10 m by 10 m, both in the aquifer and the caprock. The size of element increases progressively away from the well up to a size of 80 m by 80 m in the limit of the unstructured mesh. The structured mesh consists of elements of 25 m by 900 m in the aquifer and of 80 m by 900 m in the caprock. As a first step, a steady-state calculation is carried out to ensure equilibrium for the pressure and stress fields.

3. Caprock stability

3.1. Effect of the initial stress state

The initial stress state determines how the stress changes in the caprock as a response to fluid pressure evolution during CO_2 injection. Fluid pressure immediately increases in the aquifer as a response to CO_2 injection. However, it

drops at the beginning of injection in the caprock (Fig. 2). This occurs because of mechanical effects, such as dilation and bending of the caprock. This initial drop in fluid pressure displaces the Mohr circle to the right (Soil mechanics sign criterion is used for representation of results, i.e. stress is positive in compression). The subsequent fluid pressure increase displaces the Mohr circle to the left because the effective stresses are reduced. In addition to this, the size of the Mohr circle varies because the horizontal stress increases as a result of lateral confinement. The Morh circle becomes smaller if the horizontal stress is lower than the vertical stress because the minimum principal effective stress (horizontal stress) increases and approaches the maximum principal effective stress (vertical stress), which remains constant (Fig. 2a). Alternatively, the Mohr circles increases in size if the horizontal stress is higher than the vertical stress because the minimum principal effective stress (vertical stress) remains constant while the maximum principal effective stress (horizontal stress) becomes bigger (Fig. 2b).
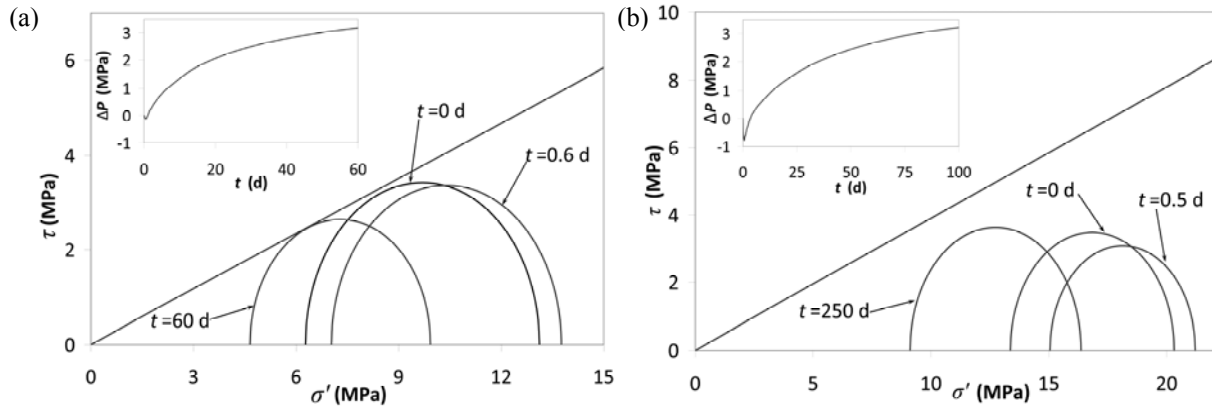

Figure 2. Stress state evolution represented by Mohr circles in a point of the caprock close to the injection well for (a) horizontal stress lower than vertical stress and (b) horizontal stress higher than vertical stress. Note that the initial pressure drop in fluid pressure (see inlet) displaces the circle to the right, but the subsequent overpressure moves the circle to the left, approaching the failure criterion. Note also that the changes in horizontal stress caused by lateral confinement change the circle size.

The plastic strain propagation pattern depends on the initial stress state. Figure 3 displays the plastic strain after 250 days of injection. Plastic strain propagates through the entire caprock if the horizontal stress is lower than the vertical stress. Thus, CO_2 may find an escape path through fractures. However, plastic strain concentrates in the contact between the aquifer and the caprock if the horizontal stress is higher than the vertical stress. If the contact between the aquifer and the caprock yields, the caprock capillary barrier may break down. If this were to occur, CO_2 would penetrate into the caprock, reducing dramatically the pH. Thus, geochemical reactions should be investigated to assess whether dissolution or precipitation dominates.
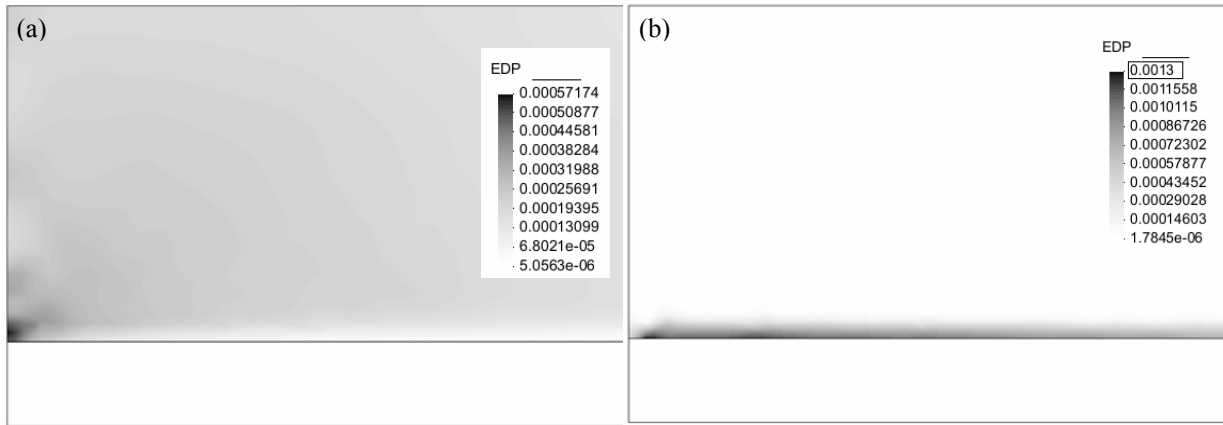
Figure 3. Plastic strain after 250 days of injection for (a) horizontal stress lower than vertical stress (plastic strain propagates through the whole thickness of the caprock) and (b) horizontal stress higher than vertical stress (plastic strain propagates horizontally in the contact with the aquifer). Only the first 700 m in the radial direction are shown.

3.2. Effect of caprock permeability

The permeability of the caprock affects fluid pressure evolution, both in the aquifer and the caprock. Brine can leak through relatively permeable caprocks ($k \geq 10^{-18}$ m^2), reducing the pressure buildup in the aquifer. Furthermore, the distance affected by the pressure perturbation grows with the square root of the permeability. Thus, the higher the permeability, the larger the volume of the caprock affected by pressure buildup. Fluid pressure, in turn, affects the displacement vector. Figure 4 shows the vertical displacement for two caprock permeabilities. The vertical displacement presents a maximum that increases and is displaced upwards with time in both cases. Volumetric compression of the upper part of the caprock occurs for low-permeability caprocks and at early times of injection in relatively permeable caprocks. This is because the caprock acts as a plate that bends because of the overpressure caused by CO$_2$ injection. Unlike the lower part of the caprock, which is horizontally compressed, the upper part of the caprock undergoes horizontal extension.
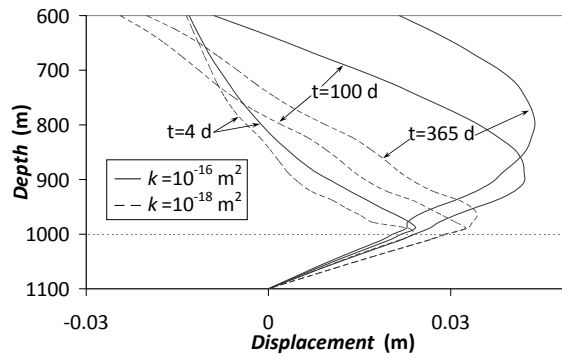

Figure 4. Vertical displacement next to the injection well at various injection times and caprock permeabilities. A low-permeability caprock limits the vertical displacement and even produces settlement in its upper part. The dotted line indicates the contact between the aquifer and the caprock.

3.3. Effect of the outer hydraulic boundary condition

Aquifers surrounded by low-permeability boundaries experience an additional overpressure once the pressure buildup cone reaches the boundary. However, fluid pressure does not evolve uniformly in the whole aquifer. While it increases close to the outer boundary, it drops in the vicinity of the injection well (Fig. 5b), which is filled with less viscous CO_2. Figure 5a displays the q-p' (deviatoric stress-mean effective stress) trajectory (this is an alternative way to analyze the failure condition) of a point of the caprock when injecting CO_2 in an aquifer surrounded by a low-permeability boundary and with horizontal stress lower than vertical stress. The initial state is represented by point A. The fluid pressure drop that occurs at early injection times in the caprock (Fig. 2) results in a higher mean effective stress (point B). Afterwards, fluid pressure increases progressively (the mean effective stress is reduced) and the horizontal stress increases because of lateral confinement (the deviatoric stress, is reduced because the maximum and minimum principal stresses become closer (see Section 3.1)). The most critical state (point C) is reached after 60 days of injection. The caprock yields at this point, because it touches the yield surface (dashed line). Thereafter, the stress state diverges slightly from the yield surface, until point D is reached. Then, the mean effective stress begins to increase, resulting in a safer situation. This change in the mean effective stress is due to the fact that fluid pressure begins to drop (after 620 d of injection). Despite a fluid pressure increase of 0.75 MPa in the outer boundary after 5 years of injection, fluid pressure in the caprock close to the injection well does not increase, but rather decrease.
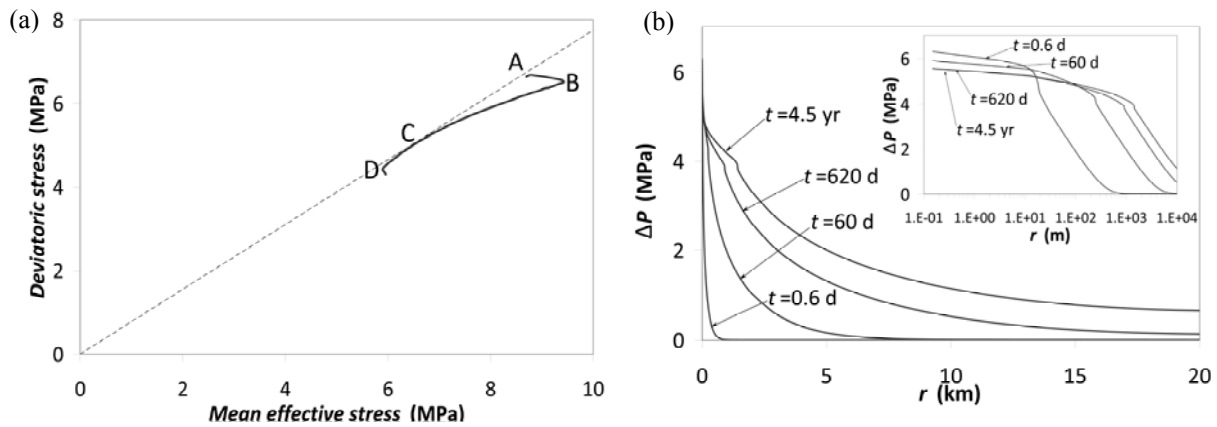

Figure 5. (a) *q*-*p'* trajectory of a point of the caprock close to the injection well for horizontal stress lower than vertical stress in an aquifer surrounded by a low-permeability boundary. The dashed line represents the yield surface. Point A shows the initial state, B is reached after the initial pressure drop, C is the most critical state (60 d) and D coincides with the time at which fluid pressure begins to drop (620 d). (b) Fluid overpressure evolution at the contact aquifer-caprock as a function of the distance to the injection well. Note that although fluid pressure increases in the outer boundary once the pressure buildup cone reaches it, pressure drops in the vicinity of the injection well (see inlet).

4. Conclusions

The main conclusions that can be drawn from this study are:

- The initial stress state controls the plastic strain propagation pattern. If horizontal stress is lower than vertical stress, plastic strain may propagate through the entire thickness of the caprock and may facilitate CO_2 migration. If horizontal stress is higher than vertical stress, plastic strain concentrates in the contact between the aquifer and the caprock, which may break the caprock capillary barrier.
- The caprock acts as a plate that bends. Thus, its upper part undergoes horizontal extension, which produces vertical compression. This may cause settlement instead of uplift in low-permeability caprocks ($k \leq 10^{-18}$ m^2) at early times of injection.
- While fluid pressure increases close to low-permeability boundaries once the pressure buildup cone reaches it, fluid pressure drops in the vicinity of the injection well due to the lower viscosity of CO_2. Thus, semi-closed

aquifers may not be critical from the mechanical point of view, but interesting because the amount of brine that migrates out of the aquifer is reduced with respect to open aquifers.

Acknowledgements

References

- [1] Rutqvist, J., Vasco, D.W. & Myer, L., 2010. Coupled reservoir-geomechanical analysis of CO_2 injection and ground deformations at In Salah, Algeria. Int. J. Greenhouse Gas Contr., 4 (*2*), 225–30.
- [2] Ferronato, M., Gambolati, G., Janna, C. & Teatini, P., 2010. Geomechanical issues of anthropogenic CO_2 sequestration in exploited gas fields. Energy Convers. Manage., 51, 1918–28.
- [3] Rutqvist, J., Birkholzer, J. T., Cappa, F. & Tsang, C-F., 2007. Estimating maximum sustainable injection pressure during geological sequestration of CO_2 using coupled fluid flow and geomechanical fault-slip analysis. Energy Convers. Manage., 48, 1798–1807.
- [4] Vidal-Gilbert, S., Nauroy, J-F. & Brosse, E., 2009. 3D geomechanical modelling for CO_2 geologic storage in the Dogger carbonates of the Paris Basin. Int. J. Greenhouse Gas Contr., 3, 288–99.
- [5] Vilarrasa, V., Bolster, D., Olivella, S. & Carrera, J., 2010. Coupled Hydromechanical Modeling of CO_2 Sequestration in Deep Saline Aquifers. Int. J. Greenhouse Gas Contr., doi:10.1016/j.ijggc.2010.06.006.
- [6] Streit, J.E. & Hillis, R.R., 2004. Estimating fault stability and sustainable fluid pressures for underground storage of CO_2 in porous rock. Energy, 29, 1445–56.
- [7] Rutqvist, J., Birkholzer, J. T. & Tsang, C-F., 2008. Coupled reservoir–geomechanical analysis of the potential for tensile and shear failure associated with CO_2 injection in multilayered reservoir–caprock systems. Rock Mech. Min. Sci., 45, 132–43.
- [8] Birkholzer, J. T., Zhou, Q. & Tsang, C-F., 2009. Large-scale impact of CO_2 storage in deep saline aquifers: A sensitivity study on pressure response in stratified systems. Int. J. Greenhouse Gas Contr., 3, 181–94.
- [9] Zhou, Q., Birkholzer, J., Tsang, C-F. & Rutqvist, J., 2008. A method for quick assessment of CO_2 storage capacity in closed and semi-closed saline formations. Int. J. Greenhouse Gas Control, 2, 626–39.
- [10] Vilarrasa, V., Bolster, D., Dentz, M., Olivella, S. & Carrera, J., 2010. Effects of CO_2 Compressibility on CO_2 Storage in Deep Saline Aquifers. Transp. Porous Media, doi:10.1007/s11242-010-9582-z.
- [11] Zienkiewicz, O. C. & Cormeau, I. C., 1974. Viscoplasticity, plasticity and creep in elastic solids: a unified numerical solution approach. *Int. J. Numer. Methods Engng 8*, 821–45.
- [12] Zienkiewicz, O. C. & Taylor, R. L., 2000. The finite element method. Vol 2: Solid mechanics. Oxford: Butterworth-Heinemann.
- [13] Olivella, S., Carrera, J., Gens, A. & Alonso E. E., 1994. Non-isothermal multiphase flow of brine and gas through saline media. Transp. Porous Media, 15, 271–93.
- [14] Olivella, S., Gens, A., Carrera, J. & Alonso E. E., 1996. Numerical formulation for a simulator (CODE_BRIGHT) for the coupled analysis of saline media. Eng. Computations, 13, 87–112.